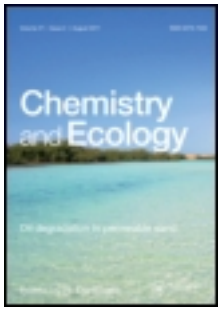

Chemistry and Ecology
Publication details, including instructions for authors and subscription information:
http://www.tandfonline.com/loi/gche20

Comparative quantitative structure-activity relationship (QSAR) study on acute toxicity of triazole fungicides to zebrafish

Feng Ding [a], Jing Guo [b], Wenhua Song [b], Weixuan Hu [b] & Zhen Li [b]

[a] College of Environmental Science and Engineering, Nankai University, Tianjin, P.R. China

[b] School of Environmental and Chemical Engineering, Tianjin Polytechnic University, Tianjin, P.R. China

Available online: 13 Jun 2011

To cite this article: Feng Ding, Jing Guo, Wenhua Song, Weixuan Hu & Zhen Li (2011): Comparative quantitative structure-activity relationship (QSAR) study on acute toxicity of triazole fungicides to zebrafish, Chemistry and Ecology, 27:4, 359-368

To link to this article: http://dx.doi.org/10.1080/02757540.2011.585780

Chemistry and Ecology
Vol. 27, No. 4, August 2011, 359–368

Taylor & Francis
Taylor & Francis Group

Comparative quantitative structure–activity relationship (QSAR) study on acute toxicity of triazole fungicides to zebrafish

Feng Ding[a], Jing Guo[b], Wenhua Song[b]*, Weixuan Hu[b] and Zhen Li[b]

[a]*College of Environmental Science and Engineering, Nankai University, Tianjin, P.R. China;*
[b]*School of Environmental and Chemical Engineering, Tianjin Polytechnic University, Tianjin, P.R. China*

(*Received 23 August 2010; final version received 31 March 2011*)

We employed two-dimensional quantitative structure–activity relationship (2D-QSAR) and hologram QSAR (HQSAR) methods to quantitatively investigate the mechanism and active site of toxicity for *Danio rerio* exposed to triazole fungicides. Our results showed that 2D-QSAR models constructed using the energy of the lowest unoccupied molecular orbit, the net C atom charges, the octanol–water partition coefficient and the molecular shape factor had higher predictive abilities. HQSAR models containing the fragment distinctions atoms (As), bonds (Bs), chirality (Ch) and donors and acceptors (D&A) had higher reliability. It was found that 2D-QSAR results explaining the toxicity mechanism were consistent with HQSAR. In summary, the hydrophobicity and shape/size of the molecule were the important factors influencing the toxic effect of these chemicals against *D. rerio*. In addition, electron exchange may occur between these fungicides and the target. The study provided a method to evaluate the environmental risk of chemicals with a similar structure, based on the QSAR models obtained.

Keywords: triazole fungicide; zebrafish; QSAR; acute toxicity; mechanism

1. Introduction

A quantitative structure–activity relationship (QSAR) study can quantitatively describe the relationship between the molecular structure of an organic pollutant and its toxicity in order to predict unknown environmental and ecological risks [1]. The US Environmental Protection Agency and Organization for Economic Cooperation and Development (OECD) have developed software, for example EPI Suite™ and QSAR Toolbox, to meet the need to estimate the environmental hazards of chemicals using predicted toxicity data.

QSAR techniques involve the use of two- or three-dimensional descriptors to develop robust models. 2D-QSAR establishes mathematical equations comprising the activity and a variety of molecular descriptors using statistical methods that include multiple linear regression (MLR), partial least-squares and nonlinear regression in which MLR is widely used. For example, a QSAR

*Corresponding author. Email: songwenhua9316@sina.com

ISSN 0275-7540 print/ISSN 1029-0370 online

DOI: 10.1080/02757540.2011.585780
http://www.informaworld.com

study of the acute toxicity of aniline and phenol compounds to *Daphnia magna* showed that the partition coefficient was the major factor impacting toxicity on *Daphnia magna* [2]. A QSAR study of the mutagenicity and carcinogenicity of simple and α–β-unsaturated aldehydes showed that the main factors affecting toxicity included molar refractivity, the partition coefficient and the energy of the lowest unoccupied molecular orbit (E_{LUMO}) [3].

Hologram QSAR (HQSAR) is a technique that employs fragment fingerprints or molecular holograms as predictive variables of biological activity or other structurally related data. HQSAR avoids the need for the three-dimensional structure of the molecules, their binding conformations or their molecular alignments; the requirements for 3D-QSAR include comparative molecular field analysis (CoMFA) and comparative molecular similarity index analysis techniques. Currently, this technology is commonly used in the field to predict and filter the environmental behaviours and ecological toxicities of a large number of organic pollutants. For example, both HQSAR and CoMFA have been used to predict the half-lives of the hydroxyl radical reaction with substituted aromatic compounds, which are major sources of environmental pollution. These models were in good agreement with the proposed mechanism for the hydroxyl-radical oxidation of halogenated aromatic compounds in the atmosphere [4]. The mutagenicity of a series of nitro compounds to *Salmonella typhimurium* has been determined using HQSAR [5].

Because of its high efficiency, broad spectrum, low toxicity and long effectiveness, triazole, a type of systemic fungicide, is widely used in agriculture for to treat powdery mildew and rust. Triazole can restrain the demethlyation of 2,4-dihydrogen-lanosterol, an intermediate in ergosterol biosynthesis. Ergosterol, the basic component of fungal cell membranes, plays an important role in the permeability of the cell. Without it, membrane structure and function disappear and lead to the death of the fungi. However, in recent years, some triazole residues have been found in agricultural products (including fruits, wheat, tea leaves and wine) [6–8] and water [9,10]. These pollutants are harmful to the environment. A systematic, in-depth study of the environmental impact of these compounds, particularly their aquatic ecotoxicity and the mode of toxicity, is urgently needed.

In the past, scientists have focused on the inhibition of CYP450 in lower animal-like plants, namely yeast, exposed to triazole fungicides. Recently, literature about the acute toxicity, spontaneous activity, neurotoxicity, development physiology and genotoxicity of these chemicals to aquatic organisms and mammals has been more common [11–13]. It was found that triazole fungicides inhibit CYP450 gene expression in aquatic organisms and mammals, thus affecting their normal physiological functions [14–16].

QSAR is used not only to explore the mechanism and active site between pollutants and their targets, but also to forecast, evaluate and filter the environmental behaviour of chemicals. Thereby, the risk of chemicals to the environment and the need for complex experiments are reduced. In this article, in order to provide a theoretical basis for reducing environmental risk, we used 2D-QSAR and HQSAR methods to quantitatively investigate the mode of toxicity and active site on zebrafish (*Danio rerio*) exposed to triazole fungicides.

2. Materials and methods

2.1. *pI$_{50}$ data*

The acute toxicities of 17 triazole fungicides to zebrafish (*D. rerio*) at 96 h post exposure, expressed as the median lethal concentration (LC_{50}), were determined, according the guidelines of OECD method 203, as reported in the literature [17]. Acute toxicity data were used to develop QSAR models. LC_{50} values were expressed as pI_{50} ($-\mathrm{Log}_{10}LC_{50}$).

2.2. *Computational details*

The variables in this 2D-QSAR study were calculated using the Gaussian03W program (Gaussian, Inc., Wallingford, CT, USA) with the HF method and 6-31G* basis set. The molecular structures and atomic serial numbers used for the calculations are shown in Table S1 (available online only). We selected the energy of the highest occupied molecular orbit (E_{HOMO}), the energy of the lowest unoccupied molecular orbit (E_{LUMO}), the net charge of nitrogen atoms in the traizole ring (Q_N) and the net charge of the C1 atom (Q_{C1}), the dipole moment (μ), the octanol–water partition coefficient (ClogP) and the molecular shape factor (ShpC) as the independent variables. A test set comprising the compounds uniconazole and tricyclazole and a training set including other compounds were considered. The parameters used in the correlation equation were related to the toxic activity. MLR of 2D-QSAR study was run on a PC using SPSS16.0 for Windows (SPSS Inc., Illinois, USA). The statistically significant correlation equation obtained from MLR to describe 2D-QSAR analysis is given below.

Analyses of the models and calculations of HQSAR were performed using SYBYL 8.1 (Tripos Inc., St. Louis, MO, USA). Holograms were created using the standard default parameters of SYBYL 8.1. Fragment distinctions included atoms (As), bonds (Bs), connections (Cs), donors and acceptors (D&A), hydrogen atoms (H) and chirality (Ch). Simultaneously, holograms were generated according to the different hologram lengths (HL) because fragment size parameters control the lengths of fragments included in the hologram fingerprints (default values ranged from 4 to 7). All other parameters were retained in their respective default positions. The HQSAR models were obtained using the following four steps: (1) hologram PLS analysis of the descriptors and the bioactivity data was calculated using the SAMPLE function; (2) the robustness of the model was validated using the leave-one-out cross-validation method; (3) based on the quality of the models produced, the best optimal number of components and the lowest standard errors were selected; and (4) cross-validated correlation coefficients and noncross-validated standard errors were obtained. A test set was developed containing bitertanol and difenocanazole. All others comprised a training set. The fragment sizes used were 1–3, 4–7, 1–10, 2–9 and 3–8. The optimal HQSAR model was derived by screening different combinations of fragment distinctions and hologram length [18].

3. Results and discussion

3.1. *Parameters for construction model*

The parameters used in the correlation equation related to the toxic activity among the candidate variables in the training set are shown in Table 1. As shown in Table 1, the parameters for tricyclazole (Compound 17), such as ClogP, E_{LUMO}, Q_N and Q_{C1}, were very different from those of the other compounds. These may make the predicted LC_{50} of tricyclazole on *D. rerio* quite different from the experimental value. The experimental pI_{50} value for each compound was compared with the predicted pI_{50} values obtained with the QSAR models.

3.2. *2D-QSAR models*

The robustness of the 2D-QSAR model is verified by the noncross-validated regression coefficient squared (R^2) and cross-validated regression coefficient squared (R^2_{cv}). Values of R^2 and R^2_{cv} closer to 1 indicate that the 2D-QSAR model has greater robustness. Predictive ability should be assessed comprehensively by four items such as R^2_{cv}, standard error (SE), F-test value, and the residual analysis chart.

Table 1. Variables used in the 2D-QSAR study.

No.	ShpC	ClogP	E_{HOMO} (a.u.)	E_{LUMO} (a.u.)	Q_{N1}	Q_{N2}	Q_{N3}	Q_{C1}	μ (Debye)
1	0.80	2.97	−0.3278	0.1338	−0.48	−0.30	−0.55	0.63	3.200
2	0.80	3.74	−0.3406	0.1183	−0.51	−0.28	−0.55	0.59	2.252
3	1.00	4.01	−0.3033	0.1245	−0.47	−0.29	−0.55	0.61	2.823
4	0.80	3.20	−0.3333	0.1327	−0.45	−0.30	−0.55	0.26	2.908
5	0.80	3.23	−0.3180	0.1264	−0.47	−0.29	−0.54	0.28	0.117
6	0.80	3.95	−0.3436	0.1116	−0.48	−0.29	−0.54	0.34	1.469
7	0.83	3.26	−0.3300	0.1275	−0.44	−0.26	−0.55	0.32	2.919
8	0.80	2.28	−0.3253	0.1332	−0.43	−0.34	−0.55	0.30	4.227
9	0.80	3.97	−0.3414	0.1105	−0.42	−0.33	−0.55	0.31	3.668
10	0.80	3.04	−0.3318	0.1282	−0.42	−0.34	−0.55	0.30	2.122
11	1.00	3.85	−0.3457	0.1120	−0.44	−0.27	−0.56	0.34	3.778
12	0.80	4.37	−0.3428	0.1105	−0.42	−0.29	−0.55	0.32	3.045
13	1.00	5.84	−0.2797	0.1218	−0.48	−0.30	−0.59	−0.72	6.292
14	0.80	1.43	−0.3517	0.1079	−0.43	−0.30	−0.54	0.35	3.596
15	1.00	3.09	−0.3309	0.1285	−0.43	−0.28	−0.55	0.33	5.287
16	1.00	3.28	−0.3353	0.1086	−0.40	−0.31	−0.55	−0.02	2.466
17	1.00	1.84	−0.2447	0.2396	−0.26	−0.17	−0.20	0.10	5.991

Notes: The atomic serial numbers of nitrogen and carbon atoms used in the calculations are shown in Table S1 (available online only).

Table 2. Statistical summary of the 2D-QSAR models.

Model	*n*	R^2	R^2cv	SE	*F*
1	15	0.739	0.682	0.202	36.887
2	15	0.919	0.857	0.118	67.628
3	15	0.925	0.844	0.118	45.234
4	15	0.943	0.889	0.103	60.327

Notes: *n*, the number of compounds contributing to building QSAR models; R^2, noncross-validated regression coefficient square; R^2_{cv}, cross-validated regression coefficient square; SE, standard error of the estimate; *F*, the value of F-test.

It was found that E_{LUMO} had a higher correlation with the toxic activity than the other physicochemical parameters (Equation (1); $R^2_{cv} = 0.682$). Combinations of E_{LUMO} and the other parameters, including Q_{C1}, ClogP and ShpC (Equations (2)–(4)), with higher predictive abilities ($R^2_{cv} > 0.800$) were obtained. The statistical results for QSAR obtained using the MLR of the training set are given in Table 2.

$$pI_{50} = -33.677E_{LUMO} + 3.153 \quad (1)$$

$$pI_{50} = -31.472E_{LUMO} - 0.509Q_{C1} + 3.032 \quad (2)$$

$$pI_{50} = -31.122E_{LUMO} - 0.451Q_{C1} + 0.037\text{ClogP} + 2.845 \quad (3)$$

$$pI_{50} = -31.137E_{LUMO} - 0.428Q_{C1} + 0.675\text{ShpC} + 2.382 \quad (4)$$

where E_{LUMO} is the energy of lowest unoccupied molecular orbit, Q_{C1} is the net charges of the C1 atom, ClogP is the octanol–water partition coefficient and ShpC is the molecular shape factor.

As shown in Table 2, compared with Equation (1), the reliabilties of Equations (2)–(4) were increased because they considered other factors that may affect the toxicity of triazde fungicides to *D. rerio*. Among these, Equation (4) with the highest R^2_{cv} value and the lowest SE consisted of E_{LUMO}, Q_{C1}, and ShpC. QSAR analysis results given in Table 2 demonstrated that Equation (4) was statistically significant. The goodness-of-fit of Equation (4) had a high R^2_{cv} value (0.889) and a small SE (0.103), with an overall *F*-test value of 60.327 at the significance level of $p < 0.05$. Therefore, in order to facilitate comparison with the HQSAR results, Equation (4) is described as Model A in the following. In addition, E_{LUMO} expresses the ability of the molecule to accept

electrons from the donor. ShpC and ClogP are related to the stereoscopic and hydrophobic effects, respectively. The results indicated that 3D-QSAR, comprising a steric field, electrostatic field and hydrophobic field, may have a high degree of fit and high predictive ability.

3.3. *HQSAR models*

The quality of the HQSAR model can be optimised by changing the fragment factor and length. The fragment factor expresses the topology mapped by the molecular hologram. In this article, several alignments of the fragments used were made. The reliability of HQSAR models is based on the cross-validated coefficient (q^2). In addition, the statistical significance of the models was described by the SE value computed according to the definitions given in SYBYL. The final model was constructed with the optimum number of components, i.e. that yielding the highest value of q^2. The predictability of a model is acceptable when $q^2 > 0.500$. Different HQSAR models ($q^2 > 0.500$) were developed and are listed in Table 3.

As shown in Table 3, among these HQSAR models, the q^2 value for models constructed only of As with five different fragment sizes were all >0.500. Two models were found to be the best statistically having q^2 values >0.630. The first had the As alignment and a fragment size of 4–7. This model had the following characteristics: $q^2 = 0.650$, SE = 0.277, HL = 71 and ONC = 6. The second comprosed the As + Ch alignment and the fragment size was 3–8. This model had the following characteristics: $q^2 = 0.639$, SE = 0.266, HL = 59, ONC = 4. The SE value of the second model was lower than that of the first. So, the second model was named Model B to facilitate subsequent analysis and discussion.

The Ch fragment involved in building the HQSAR model indicated that 3D-QSAR models for the acute toxicity of traizole fungiceds against *D. rerio* consisting of the molecular chirality and steric field may have high predictive ability, which was consistent with the 2D-QSAR results.

3.4. *Evaluation of model quality*

The acute toxicities of 17 traizole compounds against *D. rerio* were predicted using Models A and B. The experimental and predicted pI_{50} values are listed in Table 4 to verify the predicative ability of the QSAR models.

Plots of the predicted versus experimental pI_{50} values for the training and test sets in Models A and B are shown in Figure 1a ($R^2 = 0.9427$, where R^2 represents the square of the linear correlation coefficient, predicted versus experimental pI_{50} of training set) and Figure 1b ($R^2 = 0.9650$), respectively. For the chemicals that comprised the test set in Model A, the predicted pI_{50} value of

Table 3. HQSAR models of different fragment distinctions and sizes.

Fragment distinction	Fragment size	q^2	SE	HL	ONC
As	1–3	0.564	0.292	61	4
	4–7	**0.650**	**0.277**	**71**	**6**
	1–10	0.606	0.315	83	6
	2–9	0.615	0.291	257	5
	3–8	0.589	0.321	83	6
As + Bs	1–3	0.614	0.311	151	6
As + Ch	**3–8**	**0.639**	**0.266**	**59**	**4**
As + D&A	3–8	0.593	0.299	71	5
As + Bs + Ch	1–3	0.614	0.311	151	6

Note: Fragment distinction: As, atoms; Bs, bonds; Cs, connections; H, hydrogen atoms; Ch, chirality; D&A, donor and acceptor. q^2, cross-validated correlation coefficient; SE, non cross-validated standard error; HL, hologram length; ONC, optimal number of components. Values in bold represent the model with $q^2 > 0.630$.

Table 4. Experimental versus predicated pI_{50} of triazoles against *Danio rerio* via Model A and Model B.

No.	pI_{50} (exp)[a]	pI_{50}(pre)[b]			
		Model A	Res[c]	Model B	Res
1	−1.373	−1.514	0.141	−1.334	−0.039
2	−1.140	−1.014	−0.126	−1.172	0.032
3	−1.025	−1.081	0.056	−1.339	0.314
4	−1.313	−1.321	0.008	−1.172	−0.141
5	−1.063	−1.134	0.071	−1.058	−0.005
6	−0.640	−0.698	0.058	−0.646	0.006
7	−1.043	−1.165	0.122	−1.186	0.143
8	−1.574	−1.354	−0.220	−1.564	−0.01
9	−0.667	−0.651	−0.016	−0.735	0.068
10	−1.224	−1.198	−0.026	−1.228	0.004
11	−0.645	−0.576	−0.069	−0.557	−0.088
12	−0.626	−0.656	0.030	−0.569	−0.057
13	−0.386	−0.427	0.041	−0.518	0.132
14	−0.541	−0.587	0.046	−0.582	0.041
15	−1.099	−1.085	−0.014	−1.117	0.018
16	−0.348	−0.316	−0.032	−0.377	0.029
17	−1.061	−4.446	3.385	–	–

Note: [a]Experimental pI_{50}. [b]Predicted pI_{50} via Model A and Model B. [c]Res, pI_{50}(exp)-pI_{50}(pre).

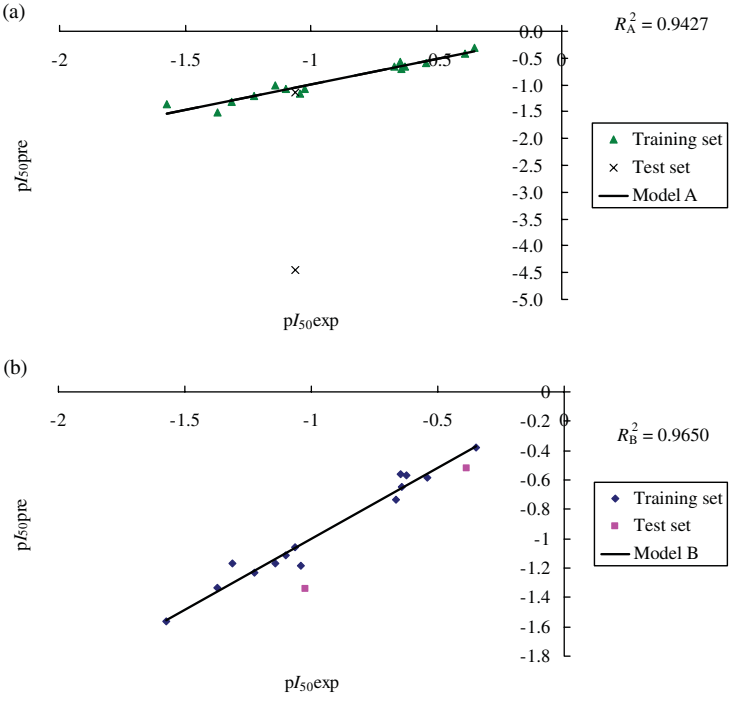

Figure 1. Plots of predicted versus experimental pI_{50} for Model A (a) and Model B (b).

paclobutrazol (Compound 4) was close to the experimental value. As can be seen from Figure 1a and Table 4, the residual error between the predicted and experimental pI_{50} values for tricyclazole is larger than for the other chemicals. The point for tricyclazole was far from the regression line. This is possibly because tricyclazole has a larger and different structure and parameters compared with the other compounds tested, leading to the large error. The results showed that the 2D-QSAR

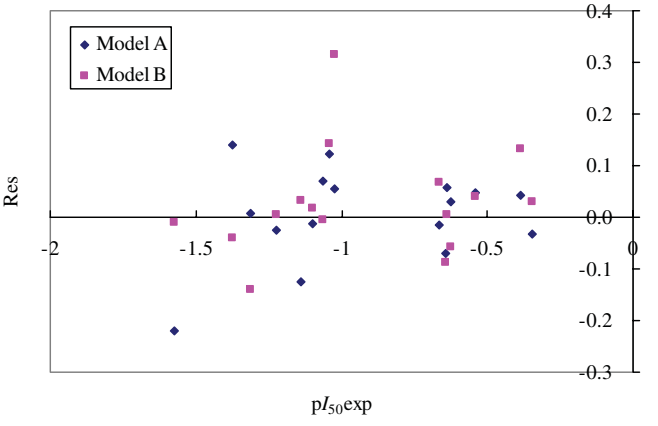

Figure 2. Plot of experimental pI_{50} versus residue based on Model A and Model B.

model established in this article could not be used to forecast the acute toxicity of compounds having a similar structure to tricyclazole. Tricyclazole was therefore excluded from the HQSAR analysis. For the Model B test set, the predicted pI_{50} value of difenocanazole (Compound 13) was close to the experimental value. However, the residual error for bitertanol (Compound 3) was a little larger (Figure 1b). Other points lie near the consensus line (Figure 1a and b). These values suggested a good conventional statistical correlation, as shown in Figure 1, and satisfactory predictive ability for Models A and B.

Experimental pI_{50} values versus the residue, based on Models A and B (except tricyclazole), are shown in Figure 2. It is shown in Figure 2 that all points are randomly distributed on the Res = 0 horizontal side indicating that Models A and B were comparatively stable and the heteroscedasticity did not exist. Therefore, Models A and B have a high degree of fit and predictive ability, and can be used to predict pI_{50} values for *D. rerio* at 96 h for chemicals with a similar structure to these triazole fungicides.

3.5. *Analysis of toxic mechanism*

At the molecular level, the toxicity of organic pollutants can be approximately divided into types, narcotic and reactive [19]. The theory is that toxic chemicals can penetrate the lipid double-layer structure of the membrane. When the concentration of a chemical is sufficient, reversible narcotic toxicity is generated because the ion channels are blocked by the toxin and damage to the normal metabolism in the cell occurs [20]. Narcotic toxicity is proportional to the lipid solubility of the chemical. However, narcotic toxicity does not depend on a special chemical structure for the pollutants. In reactive toxicity, substituted groups in the chemicals undergo a chemical or physical reaction with particular positions in an organism, including protein, enzyme and DNA, resulting in reversible or irreversible toxicity. These chemical or physical reactions include hydrogen bonding, electrophilic activity between the chemical and electron-rich nucleophilic positions located in the active sites, conjugation between the aromatic groups in pollutants and biomacromolecules, etc. Therefore, reactive toxicity is closely related to the structure of a chemical, that is, this toxicity is specific.

The bioactivities of organic pollutants can be predicted by the octanol–water partition coefficient. For example, it was found that this descriptor was the main factor affecting the toxicity of triazole fungicides against rainbow trout [21]. According to the statistical analysis, ClogP was positively correlated with pI_{50} in Equation (3) ($R^2_{cv} = 0.844$). Consequently, ClogP was one of

the factors influencing the toxicity of these triazole compounds to *D. rerio*, which is consistent with the literature in which it has been suggested that the octanol–water partition coefficient is related to the toxicity of aromatic hydrocarbons on aquatic organisms [22,23]. The distribution of pollutant between the aqueous phase and biofacies can be characterized by the ClogP parameter. The hydrophobicity of a pollutant was found to increase with increasing ClogP until ClogP reached a critical threshold, at which point chemicals penetrate the cell membrane more easily and are more toxic.

Exogenous compounds can reach the effect target through the cell wall and cell membrane barriers and so react with biomacromolecules. This process is influenced by the hydrophobicity of a chemical and the 3D steric effect of molecular structure. It has been shown that the toxicity of nitrogen-containing heterocyclic pyridine compounds to aquatic organisms is mostly influenced by the hydrophobicity and stereo factors, including molecular shape and size [24]. The structural information can be characterized by the molecular topology index, such as the order in which atoms link, the number of branches, the shape of the molecule and the presence of heteroatoms. The physicochemical properties and bioactivities of pollutants can be forecast efficiently using QSAR models based on this information. The reliability of the 2D-QSAR model was increased when ShpC was used in the construction of the model (Equation 4; $R^2_{cv} = 0.889$), in agreement with previous reports [24]. Therefore, it was presumed that ClogP and ShpC jointly influence the degree to which a chemical penetrates the cell membrane in a living body. Consequently, these descriptors affected the toxicity of chemicals to zebrafish. These compounds also have narcotic toxicity against zebrafish. This is consistent with the observations of Veith et al. [25] who reported that most organic pollutants are narcotic to aquatic organisms. However, ShpC and ClogP descriptors showed low correlation with pI_{50} ($R^2 = 0.212$ and 0.168, respectively), indicating that narcotic toxicity is not the major effect of these compounds in zebrafish.

Results from Equations (1)–(4) showed that E_{LUMO} was an efficient descriptor to predict the acute toxicity of these compounds in zebrafish. Chan et al. found that the thiol reactivity and rat or human hepatocyte toxicity induced by substituted *p*-benzoquinone compounds were closely related to E_{LUMO} [26]. The electrophilicity depicted by E_{LUMO} proved to be important in the toxicity of pollutants [27]. The pI_{50} values were all negatively correlated with E_{LUMO} in Equations (1)–(4) suggesting that electrophilicity increased with decreasing E_{LUMO}, resulting in an increase in the toxicity to zebrafish. This finding can be used to explain why triazoles having similar structures showed large differences in their toxicity to zebrafish. For example, compared with flutriafol ($E_{LUMO} = 0.1332$ a.u.; $pI_{50} = -1.574$), flusilazole, which has a similar sturucture, shows a decreased E_{LUMO} value (0.1086 a.u.), an increased pI_{50} value (-0.348), and higher toxicity. The E_{LUMO} value for triadimenol (0.1338 a.u., $pI_{50} = -1.373$) was higher than for triadimefon ($E_{LUMO} = 0.1183$ a.u., $pI_{50} = -1.140$). Nevertheless, the pI_{50} value of triadimenol was decreased and the toxicity was lower compared with triadimefon. R^2 of Equation (1) ($R^2 = 0.739$), individually constructed of E_{LUMO}, was higher than with other 2D-QSAR models ($R^2 < 0.300$) individually constructed of other molecular descriptors. A lower E_{LUMO} value enhances the ability of a compound to accept electrons and react more easily with nucleophilic groups in the target. Consequently, it has been suggested that the ability to accept electrons is the main factor influencing the toxicity of these compounds in zebrafish. Electron exchange may exist between these compounds and the target.

Likewise, the reliability of the model in which Q_{C1} participated was increased (Equations (2)–(4)), which indicated that the electronegativity of the R_1, R_2 and R_3 groups (Table S1 – available online only), including the abilities of electron withdrawal and release, was a major factor affecting the toxicity of these compounds.

The toxicity of triazole fungicides in zebrafish was closely related to E_{LUMO} and Q_{C1}, and therefore, these compounds may have reactive toxicity in zebrafish. The toxic effects may be divided into two stages: first, the triazoles pass through the cell membrane and accumulate in the

animal. This process may be affected by the hydrophobic parameter (ClogP) and the molecular shape index (ShpC). Second, electronic exchange occurs between the triazole and the target, which may be described by the electrical parameters (E_{LUMO} and Q_{C1}).

In HQSAR, the molecules are broken down into smaller structural fragments and these provide critical information about the activity of the compounds. As shown in Table 3, HQSAR models containing As, Bs, Ch and D&A fragment distinctions had higher reliabilities. The D&A fragment distinction indicated that electron exchange may exist between these compounds and the target, which agreed with the 2D-QSAR results. However, the Ch fragment distinction represented the molecular chirality of triazole meaning that the three-dimensional shape of molecules played a role in their reactions with biomacromolecules. This was consistent with the result of the 2D-QSAR study in which ShpC was the important factor affecting the toxicity of these chemicals on zebrafish. Generally speaking, As, Bs and Cs fragment distinctions are often used in HQSAR studies because these fragment distinctions contain the basic information that distinguishes each of the different fragments. In our study, the HQSAR model considering As and Bs had higher reliability (Table 3), as expected.

In summary, when chemicals react with biomacromolecules in zebrafish, the hydrophobicity and shape/size of the molecule are important factors that influence the toxic effect. In addition, electron exchange may occur between triazole fungicides and the target.

4. Conclusions

Since the last century, a large number of chemical substances have been released into the environment. QSAR methods have begun to be widely applied in environmental toxicology. In the field of pollutant risk assessment, the environmental behaviour and ecotoxicity of an unknown compound can be predicted, evaluated and screened based on QSAR models. At the same time, depending on the result of the QSAR study, scientists attempt to discover the interaction characteristics between the pollutant and the environment, and the mechanism of toxicity on organisms in order to provide theoretical guidance for pollutant control and blocking. The frequent application of triazole fungicides has negative impacts on biological safety and health. Therefore, it is important to study the impact of these compounds on the environment, in particular aquatic ecotoxicity and the mechanism of toxicity.

Acknowledgement

Financial support for this work was provided by the National Natural Science Foundation of China (No. 30800934 and No. 30771771).

References

[1] M.T.D. Cronin and J.C. Dearden, *QSAR in toxicology. 1. Prediction of aquatic toxicity*, Quant. Struct.-Act. Rel. 14 (1995), pp. 1–7.
[2] M.T.D. Cronin, Y.H. Zhao, and R.L. Yu. *PH-dependence and QSAR analysis of the toxicity of phenols and anilines to* Daphnia magna, Environ. Toxicol. 15 (2000), pp. 140–148.
[3] R. Benigni, L. Passerini, and A. Rodomonte, *Structure–activity relationships for the mutagenicity and carcinogenicity of simple and α–β unsaturated aldehydes*, Environ. Mol. Mutagen. 42 (2003), pp. 136–143.
[4] M. Vrtaènik and K. Voda, *HQSAR and CoMFA approaches in predicting reactivity of halogenated compounds with hydroxyl radicals*, Chemosphere 52 (2003), pp. 1689–1699.
[5] P.C. Nair and M.E. Sobhia, *Comparative QSTR studies for predicting mutagenicity of nitro compounds*, J. Mol. Graph. Model. 26 (2008), pp. 916–934.
[6] V. Kumar, S.D. Ravindranath, and A. Shanker, *Fate of hexaconazole residues in tea and its behavior during brewing process*, J. Chem. Health Saf. 11 (2004), pp. 21–25.

[7] E.R. Trösken, N. Bittner, and W. Völkel, *Quantitation of 13 azole fungicides in wine samples by liquid chromatography–tandem mass spectrometry*, J. Chromatogr. A 1083 (2005), pp. 113–119.
[8] L.C. Paraíba, *Pesticide bioconcentration modelling for fruit trees*, Chemosphere 66 (2007), pp. 1468–1475.
[9] R. Jeannot, H. Sabik, E. Sauvard, and E. Genin, *Application of liquid chromatography with mass spectrometry combined with photodiode array detection and tandem mass spectrometry for monitoring pesticides in surface waters*, J. Chromatogr. A 879 (2000), pp. 51–71.
[10] Q.X. Zhou, J.P. Xiao, and Y.J. Ding, *Sensitive determination of fungicides and prometryn in environmental water samples using multiwalled carbon nanotubes solid-phase extraction cartridge*, Anal. Chim. Acta 602 (2007), pp. 223–228.
[11] A.R. Allen and R.C. Macphail, *Bitertanol, a triazole fungicide, increases operant responding but not motor activity*, Neurotoxicol. Teratol. 15 (1993), pp. 237–242.
[12] R. Reeves, M. Thiruchelvam, E.K. Richfield, and D.A. Cory-Slechta, *The effect of developmental exposure to the fungicide triadimefon on behavioral sensitization to triadimefon during adulthood*, Toxicol. Appl. Pharm. 200 (2004), pp. 54–63.
[13] S. Groppelli, R. Pennati, F. Bernardi, E. Menegola, E. Giavini, and C. Sotgia, *Teratogenic effects of two antifungal triazoles, triadimefon and triadimenol, on* Xenopus laevis *development: craniofacial defects*, Aquat. Toxicol. 73 (2005), pp. 370–381.
[14] A.M. Vinggaard, C. Hnida, V. Breinholt, and J.C. Larsen, *Screening of selected pesticides for inhibition of CYP19 aromatase activity* in vitro, Toxicol. in Vitro 14 (2000), pp. 227–234.
[15] P.K. Chan, S.Y. Lu, J.W. Liao, C.F. Wei, Y.Y. Tsai, and T.H. Ueng, *Induction and inhibition of cytochrome P450-dependent monooxygenases of rats by fungicide bitertanol*, Food Chem. Toxicol. 44 (2006), pp. 2047–2057.
[16] D.B. Tully, W.J. Bao, A.K. Goetz, C.R. Blystone, H.Z. Ren, J.E. Schmid, L.F. Strader, C.R. Wood, D.S. Best, M.G. Narotsky, D.C. Wolf, J.C. Rockett, and D.J. Dix, *Gene expression profiling in liver and testis of rats to characterize the toxicity of triazole fungicides*, Toxicol. Appl. Pharm. 215 (2006), pp. 260–273.
[17] J. Guo, W.H. Song, F. Ding, J.Y. Zhang, Z. Li, X.Y. Chen, J.H. Zhang, and J. Lian, *Study on acute toxicity of zebrafish (*Danio rerio*) exposure to triazole fungicides*, J. Southeast Univ. (Medical Science Edition) 29 (2010), 406–409 (abstract in English).
[18] D. Chen, C.S. Yin, X.D. Wang, and L.S. Wang, *Holographic QSAR of selected esters*, Chemosphere 57 (2004), pp. 1739–1745.
[19] H.J.W. Verhaar, C.J. Van Leeuwen, and J.L.M. Hermens, *Classifying environmental pollutants*, Chemosphere 25 (1992), pp. 471–491.
[20] A.P. Van Wezel and A. Opperhuizen, *Narcosis due to environmental pollutants in aquatic organisms: residue-based toxicity, mechanisms, and membrane burdens*, Crit. Rev. Toxicol. 25 (1995), pp. 255–279.
[21] K. Knauer, C. Lampert, and J. Gonzalez-Valero, *Comparison of* in vitro *and* in vivo *acute fish toxicity in relation to toxicant mode of action*, Chemosphere 68 (2007), pp. 1435–1441.
[22] R. Altenburger, H. Walter, and M. Grote, *What contributes to the combined effect of a complex mixture?* Environ. Sci. Technol. 8 (2004), pp. 6353–6362.
[23] W.D. Marzio and M.E. Saenz, *QSARs for aromatic hydrocarbons at several trophic levels*, Environ. Toxicol. 21 (2006), pp. 118–124.
[24] M.P. Moulton and T.W. Schlutz, *Structure–activity relationships of selected pyridines II: principal components analysis*, Chemosphere 151 (1986), pp. 59–67.
[25] G.D. Veith, D.J. Call, and L.T. Brooke, *Structure–toxicity relationships for the fathead minnow*, Can. J. Fish. Aquat. Sci. 40 (1983), pp. 743–748.
[26] K. Chan, N. Jensen, and P.J. O'Brien, *Structure–activity relationships for thiol reactivity and rat or human hepatocyte toxicity induced by substituted* p*-benzoquinone compounds*, J. Appl. Toxicol. 28 (2008), pp. 608-620.
[27] J. Damborsky and T.W. Schultz, *Comparison of the QSAR models for toxicity and biodegradability of anilines and phenols*, Chemosphere 34 (1997), pp. 429–446.